Cerebral Cortex June 2008;18:1239–1252
doi:10.1093/cercor/bhm154
Advance Access publication September 17, 2007

Early Telencephalic Migration Topographically Converging in the Olfactory Cortex

Fernando García-Moreno, Laura López-Mascaraque and Juan A. de Carlos

Instituto Cajal (CSIC), Avenida del Dr Arce 37, Madrid 28002, Spain

Neurons that participate in the olfactory system arise in different areas of the developing mouse telencephalon. The generation of these different cell populations and their tangential migration into the olfactory cortex (OC) was tracked by tracer injection and in toto embryo culture. Cells originating in the dorsal lateral ganglionic eminence (LGE) migrate tangentially along the anteroposterior axis to settle in the piriform cortex (PC). Those originating in the ventral domain of this structure occupy the thickness of the olfactory tubercle (OT), whereas cells from the rostral LGE migrate tangentially into the most anterior telencephalon, at the level of the prospective olfactory bulb (pOB). Neurons from the dorsal telencephalon migrate ventrally, bordering the PC, toward olfactory structures. Two cell populations migrate tangentially from the rostromedial telencephalic wall to the OT and the PC, passing through the ventromedial and dorsolateral face of the telencephalon. Some cells from the germinative area of the rostral telencephalon, at the level of the septoeminential sulcus, migrate rostrally to the pOB or caudally to the OC. Thus, we demonstrate multiple telencephalic origins for the first olfactory neurons and each population following different migratory routes to colonize the OC according to an accurate topographic map.

Keywords: development, embryo culture, mouse, olfactory tubercle, piriform cortex, preplate, tangential migration

Introduction

During telencephalic development, cells are generated at specific sites and they migrate over different distances to reach their final destinations following radial or tangential routes. In radial migration, also known as gliophilic migration, the cells use the radial glia to facilitate their ascent (Rakic 1972), as typified by the cortical projecting pyramidal cells. On the other hand, tangential migration is mainly used by interneurons generated in the ganglionic eminences of the basal telencephalon that migrate over long distances to reach the dorsal telencephalon (DT) and settle in the cerebral cortex and hippocampus (De Carlos et al. 1996; Anderson et al. 1997; Tamamaki et al. 1997; Lavdas et al. 1999; Jiménez et al. 2002; López-Bendito et al. 2004). Similarly, the cells generated in the adult subventricular zone of the telencephalon migrate in the rostral migratory stream to reach the olfactory bulbs and differentiate into periglomerular and granular cells (Lois and Alvarez-Buylla 1994). The first postmitotic telencephalic neurons accumulate superficially in the cortical neuroepithelium to form the primordial plexiform layer (Marín-Padilla 1971) beneath the pial surface, also known as preplate (PP, Stewart and Pearlman 1987). This structure is the first recognizable stratum to form, although it is transitory and only persists for 3 days in mouse embryos (E10–E12). During this time, the PP is colonized by different cell populations (Jiménez et al. 2003), among them Cajal-Retzius and subplate cells, 2 important cell types required for the early development of the cerebral cortex (Marín-Padilla 1978; De Carlos and ÓLeary 1992). Although it is accepted that these 2 populations are the first cells generated in the cerebral cortex, we have described other cell populations that are generated at essentially the same time in the telencephalic neuroepithelium but that follow different migratory routes and express different markers. The present study provides further information on the behavior of these cell populations, which ultimately converge in the same area, the ventrolateral part of the telencephalon where the olfactory cortex (OC) is being formed. At this early stage, the development of the olfactory system commences, and although the olfactory bulb has still not evaginated, their output (mitral) cells and some interneurons of the OC have been generated (Bayer 1986; De Carlos et al. 1996; López-Mascaraque et al. 1996; Tomioka et al. 2000; Blanchart et al. 2006; Nomura et al. 2006).

OC is defined as the ventrolateral part of the telencephalon that receives direct input from olfactory bulb (OB) neurons, in addition to inputs from neocortical and limbic regions. It is a 3-layered structure, where the first layer (fibrillar layer) is exclusively occupied by axonal fibers and dendritic terminations. The second layer (layer of small pyramidal cells) is populated by different kind of cells, according to its morphology: small pyramids, semilunar cells, fusiform cells, and polygonal cells. Finally, in the third layer (layer of medium-sized pyramidal cells) have been identified medium-sized pyramids and fusiform cells (Valverde 1965). Here, we describe when and where different cell populations that form part of the olfactory system are generated. Although we cannot know, with the used methodology, what kind of neurons are differentiated from each cell population, our present results provide an important addition to our current understanding of early telencephalic neural migration, concluding that several cell populations move tangentially over long distances throughout the entire telencephalon, mainly in the upper part of the neuroepithelium. The extraordinary traffic of cell populations at early developmental stages is remarkable, and their mode of migration indicates that tangential migration is more prevalent that previously suspected.

Materials and Methods

Animals

Embryos (95) were generated from C57 pregnant mice (21) raised at the Cajal Institute, and the day of vaginal plug was defined as E0. All the procedures for handling and sacrificing the animals used in this study

were in accordance with the European Commission guidelines (86/609/CEE) and approved by the animal care and use committee of the Cajal Institute. Pregnant dams were anesthetized with Equithesin (3 ml/kg body weight) before surgery and then killed by cervical dislocation. The embryos were removed by cesarean section at different developmental stages (E10, E11, and E12), and the 95 embryos were used as follows: 70 were injected with tracers and cultured in toto (10 different experiments with 7 embryos each); 5 were sectioned in different planes and counterstained with acid thionin (0.05%, pH 4.5) to examine the cortical cytoarchitecture at the selected ages; and 20 embryos were used for immunohistochemistry studies.

Whole Embryo Culture

The procedure for the in toto embryo culture is set out in detail elsewhere (De Carlos et al. 1996; Jiménez et al. 2002; García-Moreno et al. 2007). Briefly, mouse embryos (E10, E11, and E12) were removed from the uterus and dissected out in a petri dish containing Hank's balanced solution at 37 °C under sterile conditions. The muscular uterine wall and decidua were removed, and Reichert's membrane was separated to reveal the vascularized visceral yolk sac containing the embryo. Although maintaining the integrity of the vitelline arteries and veins, the avascular side of the yolk sac was partially broken to expose the embryo. The amnion was removed and the vessels of the vitelline stalk were tucked under the tail of the embryo. Tracers were injected with the aid of a pressure device (Picospritzer, General Valve, Fairfield, CT) under a dissecting microscope (Nikon SMZ1500, Nikon Corporation, Tokyo). Subsequently, the injected embryo was transferred to a glass bottle containing 4 ml of culture medium, which was placed in an incubator for 1 day at 35 °C with continuous gassing (95% O_2, 5% CO_2). The embryos were cultured in medium containing heat-inactivated rat serum obtained by centrifugation of blood immediately after extraction from donor adult animals (3 times 100 × g every 5 min). This serum was filtered with Filtropur S 0.45 (Sarstedt, Nümbrecht) and supplemented with 1 mg/ml of glucose and antibiotic (penicillin–streptomycin, 100 IU/ml; Gibco, Grand Island, NY).

Tracers, Injection Sites, and Anatomical Considerations

Four different tracers were employed in this study: 1) a 2.5% solution of 1,1′-dioctadecyl-3,3,3′,3′,-tetra-methyl-indocarbocyanine perchlorate in dimethylformamide (DiI, Molecular Probes, Eugene, OR); 2) a 5% solution of tetra-methyl rhodamine (Rho, 3000 molecular weight, Molecular Probes); 3) 10 mM solution of carboxy-fluorescein diacetate succinimidyl ester (CFDA SE) in dimethyl sulfoxide (DMSO) (557 molecular weight, Molecular Probes); and 4) 10 mM solution of SNARF-1 carboxylic acid, acetate, succinimidyl ester in DMSO (SNARF-1, 568 molecular weight, Molecular Probes).

One or two different tracers were injected into the ventricular (germinative) zone of several regions of dorsal and ventral telencephalon (differently shadowed in Fig. 1*A*,*B*) and defined as follows: the lateral ganglionic eminences (LGE) subdivided in the rostral (rLGE), dorsal (dLGE), and ventral (vLGE) part of this structure; the DT subdivided into 3 separated regions, the rostral- (RDT), medial- (MDT), and caudal- (CDT) dorsal telencephalon; and the rostromedial telencephalic wall (RMTW) and the rostral telencephalic pole, just over the prospective olfactory bulb (pOB), at the level of the septo-eminential sulcus (SES). All these areas give rise to diverse cell populations that reach and converge in the OC.

The OC occupies the ventrolateral part of the telencephalon and consists of several structures (Fig. 1*C*): the anterior olfactory nucleus (also known as anterior OC, Haberly 2001), the piriform cortex (PC), and the lateral olfactory tract (lot, formed by the axons of mitral and some tufted cells from the OBs), which constitutes layer 1 of the PC, separating this structure from the olfactory tubercle (OT), located ventrally. Finally, the more caudal region of the ventrolateral telencephalon is the entorhinal cortex (EC; Haberly 2001; Brunjes et al. 2005).

Immunohistochemistry

Single and dual immunohistochemistry were performed in this study using the following primary antibodies: 1) Mouse–anti-Reelin (Chemicon, Temecula, CA mouse, MAB5364, Clone G10; 1:1000; 2) Rabbit–anti-calbindin-D28K (CB, Swant, Bellinzona, Switzerland; CB38, 1:10 000); 3) Polyclonal anti-calretinin antiserum (CR, Swant; 7699/4, 1:2000); 4) Mouse–anti-β-tubulin class III (TuJ1, gift from Dr Frankfurter, 1:1000); 5) Rabbit–anti-Tbr1 (Chemicon, 1:1000); 6) Guinea pig–anti-doublecortin (DCx, Chemicon, 1:5000); and 7) Mouse–anti-Glutamic Acid Decarboxylase (GAD6, DSHB, Iowa, IA; 1:2000). The secondary antibodies used in this study were: biotinylated Goat Anti-Guinea-Pig IgG (H + L) (Atom Vector, 1:200), Alexa 568 Goat Anti-Rabbit IgG (Molecular Probes, 1:2000); Alexa 568 Anti-Mouse IgG (Molecular Probes, 1:2000); Alexa 568 Streptavidin (Molecular Probes, 1:2000); Alexa 488 Streptavidin (Molecular Probes, 1:2000); Biotin-SP-AffiniPure Goat Anti-Rabbit IgG (H + L, Jackson, West Grove, PA; 1:200); and Biotin-SP-Affinipure-conjugated Goat Anti-Mouse IgG (H + L, Jackson, 1:200). All the secondary antibodies were diluted in phosphate buffer tween (PBT) containing 5% normal goat serum (NGS) and 0.1% bovine serum albumin (BSA). Cryostat sections (20 μm) were pretreated for 1 h with a solution of 5% NGS and 0.1% BSA in phosphate buffer saline (PBS, pH 7.2) containing 0.1% Tween PBT. Sections were incubated with the primary antibodies diluted in the same blocking solution overnight at 4 °C. After rinsing with PBT, the sections were incubated with the secondary antibodies for 2 h. The biotin-SP-affinipure-conjugated antibodies were developed using an avidin–biotin peroxidase complex solution, with diaminobenzidine as the peroxidase substrate (ABC Elite Kit, Vector Laboratories, Burlingame, CA). For all the antibodies, a series of control sections were stained, where the primary antibody was omitted and no specific staining was seen. The sections were mounted on gelatinized slides and counterstained with acid thionin or with bisbenzimide when using fluorescent secondary antibodies.

Data Analysis

Single- and double-injected embryos were fixed in 4% paraformaldehyde (PF) and examined under a fluorescence-dissecting microscope (Leica MZFL-III), where the whole brains were photographed. The brains were then embedded in agar, and 75-μm vibratome sections were obtained in the coronal, sagittal, or horizontal planes. Fluorescent sections were counterstained with 0.002% bisbenzimide (Hoechst 33258, Sigma, St Louis, MO) in PBS, mounted with a mixture of glycerol-phosphate buffer (PB) (1:1), and studied under a fluorescent microscope (Nikon, Eclipse E600) equipped with a digital camera (Nikon DMX 1200F) and the appropriate filter cubes: rhodamine (560–610 nm) or fluorescein (450–490 nm) to visualize DiI/Rho/SNARF-1/Alexa 568 and CFDA/Alexa 488, respectively. Bisbenzimide labeling was studied under ultraviolet illumination. Selected areas of double-labeled or DiI-labeled cells were also studied and photographed using a Leica TCS 4D confocal microscope.

Rho and CFDA-injected embryos were initially fixed in 4% PF, and their brains were postfixed in fresh 4% PF supplemented with 15% sucrose in 0.1-M PB at 4 °C for several hours. The embryos were then transferred to 30% sucrose in PB until the tissue sunk in the medium. Coronal or horizontal frozen cryostat sections (20 μm) were obtained (Frigocut N, Leica Inc., Germany) and mounted on Tespa-coated glass slides. In order to performed double immunohistochemistry, these sections were incubated with Alexa 488/568 streptavidin.

In the course of this study, we realized that the fluorescent tracers rarely label a small number of cells in transit from the nearest germinative labeled places because when we inject 2 different tracers in the same animal and one of them is injected near the migratory route labeled with the other dye, we never observed double-labeled cells (see Supplementary Fig. S1).

Note about Cell Quantification

No statistical analysis was performed on the earliest migrating cell populations originated in the different telencephalic regions selected due to the reduced number of cells labeled in each injection. Nevertheless, all the Rho and CFDA-fluorescent labeled cells were counted by fluorescence microscopy and analyzed for the expression of additional neuronal markers. Confocal microscopy helped us to resolve doubts regarding the double labeling of cells. All photographs were adjusted for contrast and brightness with Adobe Photoshop (v. 8.0, San Jose, CA).

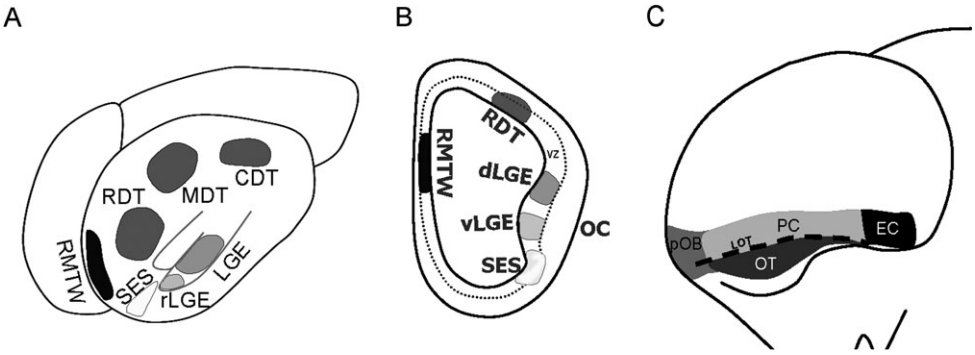

Figure 1. Diagrams showing the different telencephalic regions of an E11 mouse embryo where the tracers were injected (*A* and *B*) and the early distribution of the olfactory areas (*C*). (*A*) The shadowed areas differentiate each injection site in a view from the left-top of a translucent cartoon that also displays the internal structures, including the RMTW (black), the main body of the LGE (medium gray) and the rostral portion of this structure (rLGE, light gray), and the rostral telencephalic pole at the level of the SES (white). The dark gray shadow distinguishes the injected regions in the DT, specifically the anterior portion of the RDT, and the MDT or the CDT. (*B*) Schematic representation of a coronal section of the anterior half of the telencephalon with the localization of the different areas injected. The subpallial LGE has been subdivided in dLGE (medium gray) and vLGE (light gray). vz, ventricular zone. (*C*) Schematic representation of embryonic olfactory areas. The dashed line represents the lot. The anterior part is the pOB. The gray area above the lot is the PC and the area below is the OT. The darker area that appears caudally is the EC.

Results

Expression of Markers Used to Study Migratory Cell Populations

In the present study, we used 3 reported markers of migratory neuroblasts: DCx, a microtubule-stabilizing protein that is strongly expressed in migrating neuroblasts (Lee et al. 1990; Gleeson et al. 1999) and during differentiation (Francis et al. 1999), the calcium-binding proteins, CR and CB, that both bind to actin and tubulin filaments, structures implicated in cell movement (Hof et al. 1999).

In order to obtain a complete view of the early telencephalic expression of these proteins, we carried out immunohistochemistry on whole brains from E11 mouse embryos. At this age, the PP is forming in the upper part of the cortical neuroepithelium and numerous neuroblasts are migrating to reach their adult position in the telencephalon. Furthermore, many cells at this stage begin to accumulate in the pOB and OC.

DCx expression (Fig. 2*A–D*) is present throughout the entire telencephalic surface, although the strongest labeling was detected in the basal telencephalon, both in the mantle zones of the lateral and medial ganglionic eminences (MGEs) (Fig. 2*D*) and in the early PC (Fig. 2*B*). This labeling in the prospective OC extended toward the rostral pole of the telencephalon where the OBs will emerge (Fig. 2*C*). At the ventral telencephalic surface, the labeled cells extended throughout the PC reaching the pOB and orientating toward the lot (Fig. 2*C*).

The expression of CR followed a pattern similar to that of DCx (Fig. 2*E–H*), although the dorsal part of the neocortical mantle was weakly labeled when compared with the lateral part of the neocortex (Fig. 2*E,G*), where the labeled cells were fusiform and most of them directed their processes toward the ventral telencephalon (Fig. 2*G*). As occurred with DCx expression, the OC displayed a large number of CR-immunoreactive cells (Fig. 2*F,H*).

In contrast, the pattern of CB expression was very different to that of the other markers (Fig. 2*I–L*) because there were no labeled cells at the dorsal (NC, developing neocortex) or lateral level (PC). However, a large cell population expressing CB appeared in the mantle zone of the MGE (Fig. 2*K*) and in the olfactory region known as the OT. The most dorsal portion of this cell population extended to the PC without entering into it but rather bordering this structure (Fig. 2*K* asterisk, *L*). At the superficial level, the CB-immunoreactive (-ir) cell population displayed a rostrocaudal orientation (Fig. 2*J*). In the following days, some CB-ir cells reached the neocortical mantle, surrounding the PC and migrating tangentially through the marginal and intermediate zones.

Together these expression patterns highlighted the existence of different cell populations that reached and accumulated in several olfactory regions (pOB and OC), having followed tangential migratory routes through the telencephalon.

Early Neuronal Migration from LGE

To determine the migratory behavior of the earliest cells generated in the LGE at E10–E12, we injected different fluorescent dyes (Rho, CFDA, and DiI) at 2 different sites in the main body of this structure (dorsal and ventral), but avoiding both the rostral part (that which emerges alone in transverse sections before the MGE becomes visible) and the caudal part (from which the intereminence sulcus vanished). Alternatively, in another set of experiments, we performed injections in the rostral part of the LGE. The injected embryos were cultured in toto for 24 h, and the labeled cell populations that followed characteristic migratory pathways were analyzed as summarized in Figures 3*A,B* and 4*A,B*.

Neuronal Migration from the dLGE to the PC

Labeled cells initially follow a radial migration toward the pial surface (Fig. 3*B,D,H* and insert, *J*), and later, they spread into the anteroposterior axis of the brain by tangential migration to occupy the entire PC from the rostral (Fig. 3*F*) to the caudal telencephalic domain (Fig. 3*C*-arrowhead, *E*). Interestingly, we found more cells located caudally than rostrally, and none of the cells reached the more rostral pole at the level of the pOB, a territory that will be populated by cells generated in other structures, as in the rLGE (see below). In general, the cells generated in the dLGE did not only colonize the external part of the neuroepithelium because many cells were separated from the pial surface, occupying the thickness of the PC (Fig. 3*D–H,J,K*). All these cells were neurons that express TuJ1 (data

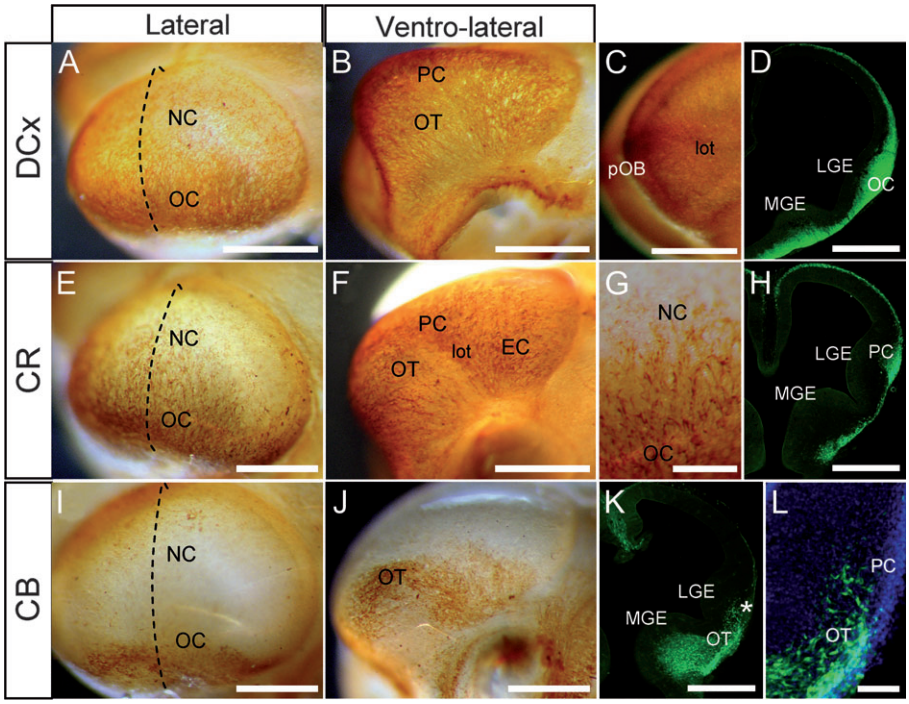

Figure 2. Immunohistochemistry of the cells undergoing tangential migration that express different markers at E11. In the pictures displaying whole brains (*A*, *B*, *C*, *E*, *F*, *I*, and *J*), rostral is left. (*A–D*) DCx immunoreactivity in a brain seen from both, a lateral (*A*, *C*) and a ventrolateral (*B*) view. Immunoreactive cells spreading over the whole telencephalic surface, with a dense accumulation in the OC and in the pOB. (*D*) Coronal section at the level of the discontinuous line in (*A*) showing the strong DCx immunoreactivity in the superficial zone of the whole telencephalon and the increased intensity in the basal telencephalon, especially throughout the OC. (*E–H*) calretinin (CR) immunoreactivity from a lateral (*D*, *G*) and ventrolateral (*E*) view. The immunoreactivity is weak in the dorsal telencephalon (developing neocortex, NC) and strong in the OC, mainly in the PC, in the lot, and in the EC. (*G*) Enlargement of the lateral telencephalic area showing the CR-ir cell disposition. (*H*) Coronal section at the level of the discontinuous line in (*E*) showing the superficial immunoreactivity in the dorsal telencephalon and the especially intense staining in the PC. (*I–L*) calbindin (CB) immunoreactivity is restricted to the basal telencephalon, in an area in front of the MGE, the OT. There is no CB labeling in the NC or in the PC. (*K*) Coronal section at the level of the discontinuous line in (*I*), showing that CB immunoreactivity is especially intense in the OT. The PC is free of any label (asterisk). (*L*) Enlargement of the OC area displayed in *K*, shows CB-ir cells surrounding the PC. The section has been counterstained with bisbenzimide. Scale bars: (*A*, *B*, *D*, *E*, *F*, *H–K*), 500 μm; (*C*, *G*), 200 μm; and (*L*), 100 μm.

not shown), and they displayed bipolar and fusiform or multipolar morphologies orientated in different planes: tangential, radial, or oblique.

There was strong expression of Reelin (Reln; Fig. 3*G*) and CR (Figs 2*D–F* and 3*H*) in the PC, and some neurons generated in the dLGE that settled in this structure expressed Reln (23.5%; Fig. 3*G,Q*) and CR (50.0%; Fig. 3*H,Q*). Furthermore, the majority of these migratory cells expressed Tbr1 (74.1%; Fig. 3*I,J,Q*). However, none of the cells generated in the dLGE expressed CB (Fig. 3*K,Q*), immunoreactivity for this protein being restricted to the OT territory at these ages (Figs 2*G–I* and 3*K*).

Neuronal Migration from the vLGE to the OT

Cells generated in the vLGE migrated radially to the mantle zone of the LGE where they spread to occupy the complete thickness of the OT (Fig. 3*L–P*). This cell population did not mix with the cells generated in the dLGE, setting down a strict separation between these 2 populations. The horizontal dispersion of these cells through the rostrocaudal axis was much more restricted than that of the cell population coming from the dLGE. All these cells expressed TuJ1 but very few expressed the other markers analyzed, such as CB (11.3%; Fig. 3*O,Q*), Tbr1 (1.2%; Fig. 3*P,Q*), and CR (1.6%; Fig. 3*L,M,Q*). None of these cells expressed Reln (0.0%; Fig. 3*N,Q*).

Neuronal Migration from the rLGE to the pOB

After fluorescent tracer injection into the rLGE, an important number of labeled cells migrated toward the rostral telencephalic pole (Fig. 4). At first, cells generated in the rLGE at E11 (Fig. 4*C*) and E12 migrated radially to the PC, and afterward, the majority of them reoriented their processes and migrated rostrally toward the pOB. This migration is roughly parallel to the horizontal axis of the brain (Fig. 4*C,D*), and when the cells reached the rostral telencephalic pole, they spread in a fan-like fashion to occupy the entire dorsoventral extension of the pOB. These cells employed the PC as a tangential migratory substratum (Fig. 4*C,D,F,G,K,L*), reaching the pOB area within the 24 h in culture. It is important to note that, after DiI injections into the medial or caudal part of the LGE, we never found neurons migrating in a rostral direction. Thus, the cells that migrated tangentially toward the pOB only seemed to be generated in the rLGE. During the migration of the cells generated in the rLGE, there is a rapid morphological transformation. First, migrating cells display a fusiform and bipolar morphology (Fig. 4*F*) with long processes extending parallel to the PC surface. As they enter the rostral areas, they separate and display a more differentiated morphology by splitting their leading processes (Fig. 4*E*).

The expression of different markers in pOB cells generated at E11–E13 in the rLGE was analyzed by immunohistochemistry in cultured embryos, after the injection of tracers (Rho, CFDA) in this structure. As expected, all cells that migrated rostrally to the pOB were neurons and accordingly expressed TuJ1. Moreover, there was strong CR expression in this prospective olfactory structure, and all the tangentially migrating cells that

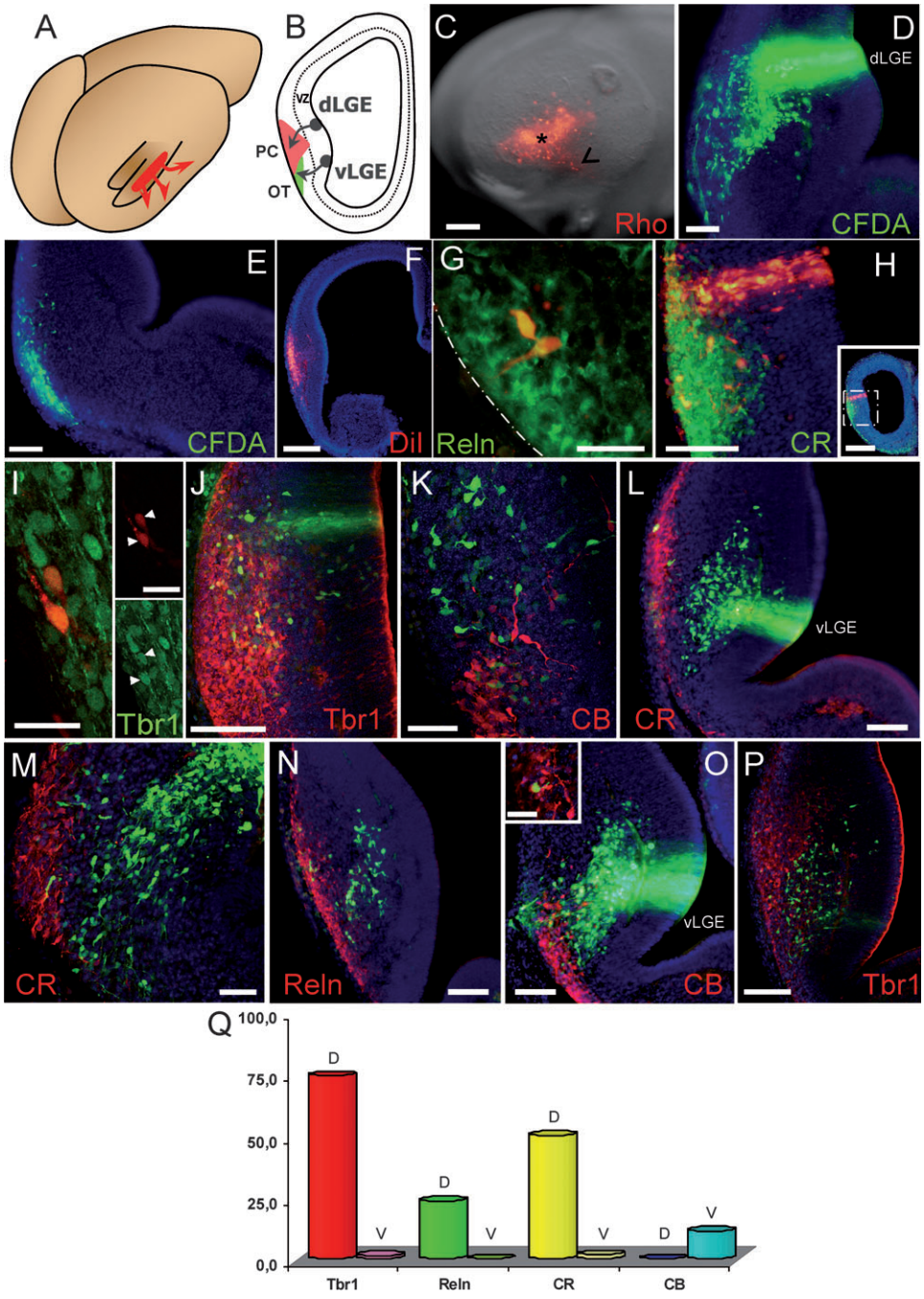

Figure 3. Neuronal migration toward the OC at E10–E12 from the main body of the LGE, subdivided into its dorsal (dLGE) and ventral (vLGE) part. (*A*) Schematic drawing showing the localization of the brain structure injected with different fluorescent markers (Rho, CFDA, or DiI) and the migratory routes that labeled cells followed toward the OC, where they spread along the rostrocaudal axis. Rostral is bottom-left, and caudal is upper-right. (*B*) Representation of a coronal section showing the injection sites in the dLGE and vLGE and the structures colonized by the labeled cells, the PC and the OT. (*C*) Lateral view of an injected brain from a E11 mouse embryo. The asterisk marks the site of the Rho injection in the dLGE. The labeled cells settle in the PC (arrowhead). (*D–F*) Coronal section of embryos injected in the dLGE with CFDA or DiI. Labeled cells reach the anterior (*F*) or posterior (*E*) PC and occupy all the deep layers of this structure. (*G*) Immunohistochemistry for Reelin (Reln, green color) in a coronal section showing 2 Reln-ir neurons (yellow–red color) in the PC coming from the injection site (double labeled). (*H*) Coronal section immunostained for calretinin (CR, green color) showing that cells originating in the dLGE (injection site, red) reach and spread into the PC (see inset for localization). Some of them express CR (yellow). (*I*, *J*) Immunohistochemistry for Tbr1 in coronal sections. The majority of the dLGE cells that reach the PC express Tbr1. Cells in (*I*) are double labeled as shown in the upper (Rho, red labeled) and the lower (Tbr1, green labeled) insets. (*K*) Coronal section immunostained for calbindin (CB, red), where the labeled cells are confined to the OT, meanwhile the cells generated in the dLGE (CFDA, green) reach the PC. (*L* and *M*) Coronal sections immunostained for calretinin (CR, red) showing the consequences of a CFDA injection in the vLGE (green). Green cells migrate toward the OT and do not mix with the red cells. (*N*) Coronal sections immunostained for Reelin (Reln, red) that do not mix with green cells that originated in the vLGE. (*O*) Coronal sections immunostained for calbindin (CB, red) shows the consequences of a CFDA injection in vLGE (green). The green cells migrate toward the OT and mix with CB-ir cells, some of which coexpress CB (inset). (*P*) Coronal sections immunostained for Tbr1 (red) showing green cells coming from vLGE that do not mix and do not express Tbr1. (*Q*) Bar diagram showing the percentage of cells expressing a given compound according to its precedence, dorsal (D) or ventral (V) LGE: Tbr1 (D, 74.1%; V, 1.2%), Reln (D: 23.5%; V: 0.0%), CR (D: 50.0%; V: 1.6%), and CB (D: 0.0%; V: 11.3%). Sections in (*D–F*), (*H*), (*J–P*) are counterstained with bisbenzimide (blue). Scale bars: (*C*, *F*) and inset in (*H*), 500 μm; (*D*, *E*, *H*, *J*, *L*, and *N–P*), 100 μm; (*G*, *K*, and *M*), 50 μm; and (*I*) and inset in (*O*), 25 μm.

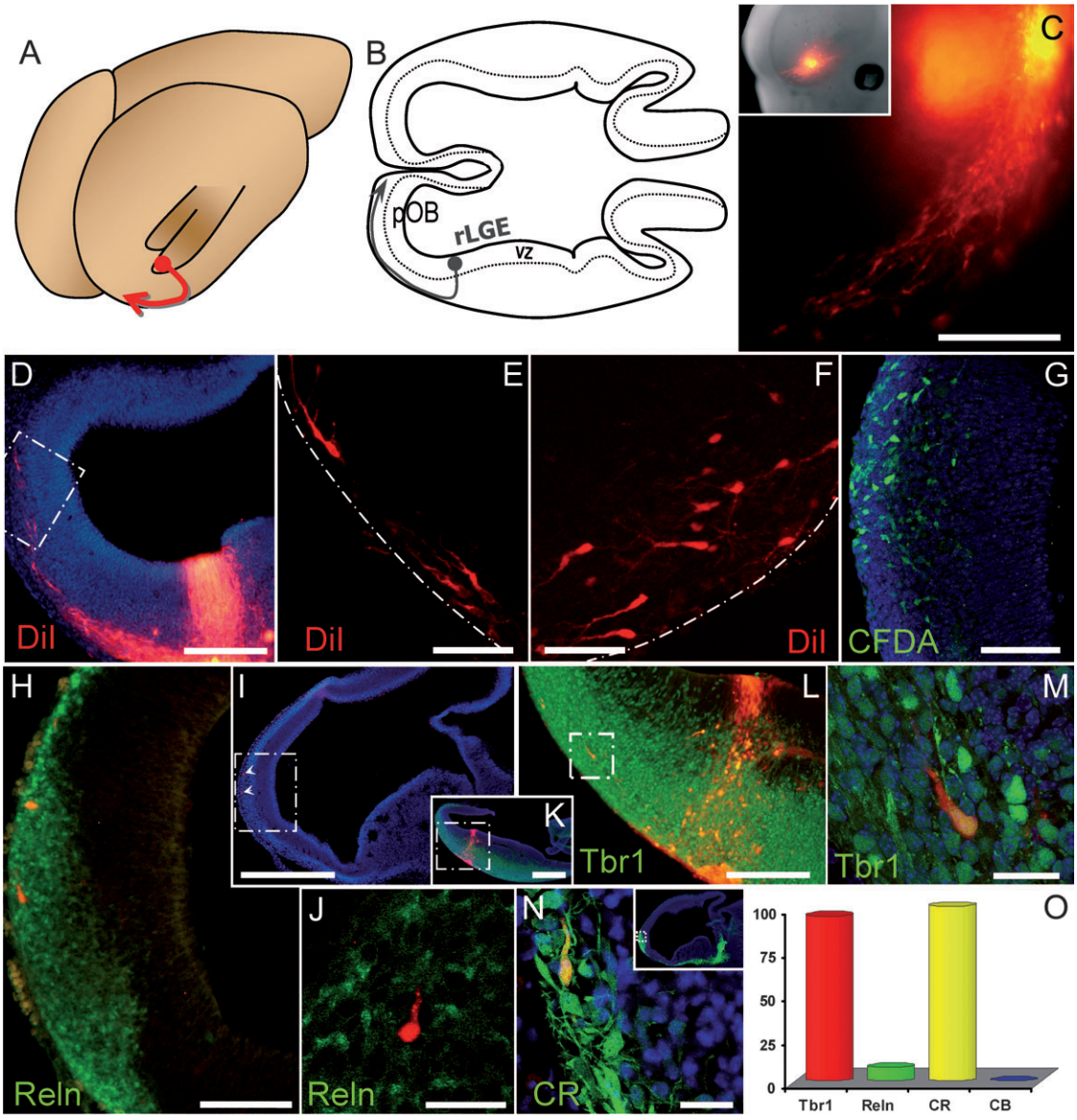

Figure 4. Neuronal migration toward the pOB at E11 from the rLGE. (*A*) Schematic drawing showing the localization of the brain structure injected with different fluorescent markers (Rho, CFDA, or DiI) and the migratory routes that the labeled cells followed toward the pOB. Rostral is bottom-left, and caudal is upper-right. (*B*) Representation of a horizontal section showing the injection site in the rLGE and the region colonized by the labeled cells (pOB). Rostral is to the left, and caudal is to the right; vz, ventricular zone. (*C*) DiI injection site in the entire brain showing the rostrotangential migration of the labeled cells. The inset shows the location of the injection in the whole embryo head. (*D*) Horizontal section from the embryo in (*C*), at the level of the LGE, showing the DiI injection site and the radial migration of the labeled cells toward the pial surface and their rostral displacement through the upper part of the neuroepithelium. The inset is enlarged in (*E*) and shows the cells that arrived at the pOB and that their leading process branched. (*F*, *G*) show cells labeled with DiI and CFDA, respectively, migrating rostrally through the PC. The different cell disposition is because (*F*, *G*) are horizontal sections, whereas (*E*) is a coronal section. (*H*) Sagittal section immunostained for Reelin (Reln, green). Positive cells occupy the entire region of pOB, where 2 Rho-labeled cells that do not express Reln appear to come from the injection site. This picture has been enlarged from that in (*I*) (box). (*J*) Example of Rho-labeled cells that do not express Reln. (*K*) Horizontal section immunostained for Tbr1 (green) following a Rho injection in the rLGE. The box is enlarged in (*L*) to show the detail of the Rho-labeled cells migrating radially to the pial surface and tangentially toward the rostral pole. Note how the Rho-labeled cells also expresses Tbr1 (yellowish color). (*M*) Amplification of the box in (*L*), showing a migrating double-labeled cell. (*N*) Sagittal section immunostained for calretinin (CR, green) shows the pOB with a double-labeled cell. This picture is an enlargement of the inset. (*O*) Bar diagram showing the percentage of cells expressing a given protein: Tbr1 (94.5%), Reln (7.8%), CR (100.0%), and CB (0.0%). The pictures (*D*, *G*, *I*, *K*, *M*, and *N*) have been counterstained with bisbenzimide (blue color). Scale bars: (*I*, *K*), 500 μm; (*C*), 250 μm; (*D*), 200 μm; (*E*, *H*, and *L*), 100 μm; (*F*, *G*), 50 μm; and (*J*, *M* and *N*), 25 μm.

reached it express this protein (Fig. 4*N*,*O*; 100.0%). However, we did not find any migrating cells that originated in the rLGE that were CB-ir or in the pOB (Fig. 4*O*). Although during early embryonic development there was strong Reln expression in the pOB (Fig. 4*H*), practically none of the cells arriving from the rLGE expressed Reln (Fig. 4*O*; 7.8%). Tbr1 is a transcription factor that is classically considered as a pallial marker, however, surprisingly, we found Tbr1 expression at all telencephalic levels and even at some subpallial regions (Fig. 4*K*,*L*). Indeed, almost all the cells that originated in the rLGE (subpallial structure) expressed Tbr1 (Fig. 4*L*,*M*,*O*; 94.5%). These subpallial cells do not express γ-aminobutyric acid (GABA) at E12, and they were not immunoreactive for GAD6 at the end of the culture.

Early Neuronal Migration from the SES

At E10–E11, tracer injections into the rostral pole of the DT at the level of the SES (Fig. 5*A*–*E*,*H*) identified a significant number

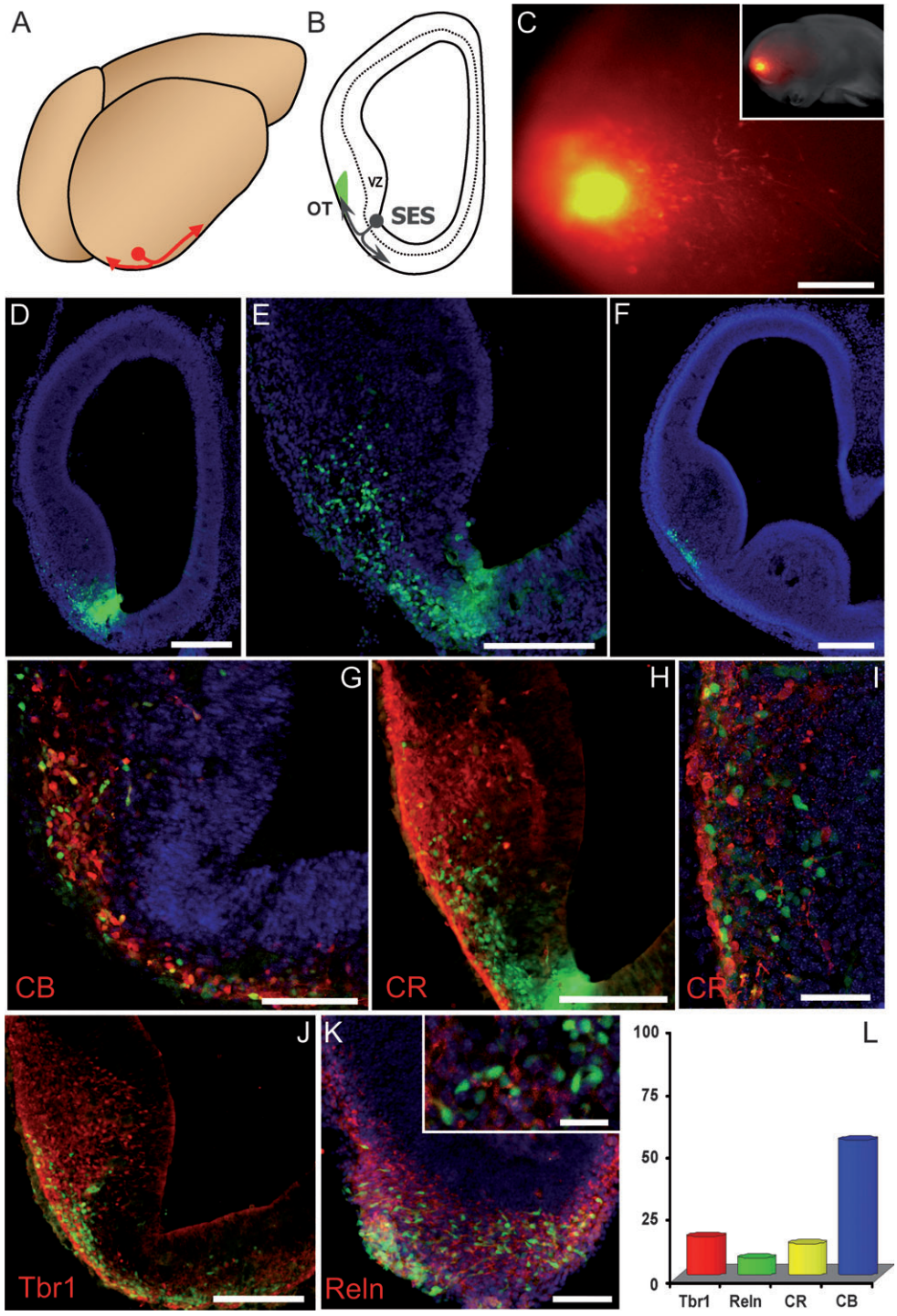

Figure 5. Neuronal migration from the rostral telencephalic pole at the level of the SES. (*A*) Schematic drawing showing the localization of the brain structure injected with different fluorescent markers (DiI, CFDA) and the migratory routes taken by the labeled cells. Rostral is bottom-left, and caudal is upper-right. (*B*) Representation of a coronal section showing the injection site in the SES and the region colonized by the labeled cells, the OT (green); vz, ventricular zone. (*C*) DiI injection site in the entire brain showing the migration of the labeled cells. The inset shows the location of the injection in bright field microscopy. (*D*) Coronal section at rostral level showing the CFDA-injection site in the SES. Some labeled cells ascend toward the OT. (*E*, *F*) Coronal sections showing the disposition of labeled cells at more caudal levels. (*G*) Coronal section displaying the CFDA-labeled cells (green) migrating from the injection site and immunostained for CB (red). Half of the migrating cells express CB. (*H*) Coronal section with CFDA-labeled cells (green) and immunostained for CR (red). (*I*) Enlargement of the OT area in a coronal section to show that CFDA-labeled cells (green) do not express CR. (*J*) Coronal section with CFDA-migrating cells occupying the OT and immunostained for Tbr1 (red) that mainly occupy the PC. (*K*) Partial view of a rostral-coronal section immunostained for Reln (red) and CFDA-labeled cells (green) showing the pOB. There are no double-labeled cells as seen in the inset. (*L*) Bar diagram showing the percentage of cells expressing a given compound: Tbr1 (15.5%), Reln (7.1%), CR (12.6%), and CB (54.5%). Pictures (*D*–*G*, *I*, and *K*) have been counterstained with bisbenzimide (blue). Scale bars: (*C*, *D*, and *F*), 250 μm; (*E*, *H*, and *J*), 200 μm; (*G*, *K*): 100 μm; (*I*) 50 μm; and inset in (*K*), 25 μm.

of migratory cell streams following different directions. Although the most prominent was initially the radial migratory pathway, tangential migration toward the more ventral part of the OC or the OT was observed later on. Indeed, injections in the SES area labeled cells that moved upward and downward in the coronal plane to colonize the entire extension of OT (Fig. 5*A–E,G–K*). Moreover, the rostrocaudal axis was also used by different cell populations that migrated tangentially. Because the PC is never occupied by cells generated in the SES, some cells moved rostrally until they reached the pOB but most of them moved caudally up to the end of the OT (Fig. 5*F*). These cells usually displayed long leading processes (Fig. 5*C*), and all the cells originating in the SES formed neurons because they all expressed TuJ1. Furthermore, 54.5% of the cells are CB positive (Fig. 5*G,L*), although a few of them express Reln (Fig. 5*K,L*; 7.1%), CR (Fig. 5*H,I,L*; 12.6%), or Tbr1 (Fig. 5*J,L*; 15.5%).

Early Neuronal Migration from the DT

The DT constitutes the neocortical neuroepithelium and tracer injections (DiI, Rho, CFDA) into the full extension of the DT-germinative zone gave rise to labeled cells that migrated ventrally to reach the OC (Fig. 6*A*). To determine whether there was any difference in cell migration throughout the entire extension of this structure, we performed tracer injections at 3 distinct sites, the rostral (RDT, Fig. 6*A–D*), medial (MDT, Fig. 6*A,E*), and the caudal part of the DT (CDT, Fig. 6*A,F*). Labeled cells from the RDT reached the OC, and although some cells migrated rostrally from there, the majority migrated caudally. Cells labeled from the MDT move caudally when they arrived at the OC, and cells labeled from CDT migrated more rostrally to reach the PC, avoiding the EC (see scheme in Fig. 6*A*). The general feature of the cells that originated from all DT regions is that the tangential migration across the PP is not entirely confined to the upper part of this stratum, but they also occupied the deeper part of this primordial layer. In this way, these cell populations do not mix with certain migratory populations that course subpially (Fig. 6*G,H*). When cells generated in the DT arrived at the level of the corticostriatal sulcus, the cell stream divided into 2 branches, an internal and an external stream that essentially bordered or occupied the deepest levels of the PC, mainly at the medial and caudal levels (Fig. 6*B,G,J*). Some DT-generated cells, migrating subpially, surpassed the PC and reached the OT. The immunohistochemical characterization identified the cells migrating from the DT as neurons due to their TuJ1 expression, and almost all of them express Tbr1 (Fig. 6*L,M*; 92.7%). It is interesting to note that, although some cells generated in the DT arrived at a CB-rich area (OT), they did not express this calcium-binding protein (Fig. 6*M*). However, some of them express Reln (Fig. 6*H,I,M*; 18.8%) and/or CR (Fig. 6*J,K,M*; 36.7%).

Early Neuronal Migration from the RMTW

Early in development (E10–E11), cell populations generated in the RMTW migrate tangentially following 2 separate (and divergent) routes to reach and settle in the OC (Fig. 7*A,B*). The RMTW is a pallial area situated in the medial wall and rostral to the cortical hem, the septum being located ventral to this region (Fig. 7*B*). Migratory cells generated in the RMTW reached the OC following 2 different and contrasting pathways: 1) a dorsal-lateral route, whereby dorsally migrating cells crossed the neocortex to reach the PC (Fig. 7*A–C,E*), and 2) a ventral-medial route, whereby ventrally migrating cells descended through the medial wall, crossing the subpallial surface to reach the OT (Fig. 7*A,B,D,F*). Tangential migrating cells using the first route crossed the dorsal and lateral pallium to reach the PC via the cortical PP. It seems that they ran somewhat rostrally, but when the cells arrived at the PC, they turned backward to follow the same caudal direction observed in migratory routes from the LGE, DT, and SES (Fig. 7*A,G*). In both cases, the cells displayed a bipolar or multipolar morphology when they reached the OC and they colonized the entire depth of this structure (Fig. 7*D,F*). The cells using the second route (ventromedial) constituted a larger population, and some of them settled in the diagonal band of Broca area (DBB; Fig. 7*H*). The rest of the ventrally migrating cells arrived at the OT, and some superficial elements reached the PC, at the level of the lot.

The cells generated in the RMTW were characterized by combining fluorescent tracers (Rho, CFDA) with immunohistochemistry for TuJ1, Tbr1, CR, CB, and Reln. As expected, all migrating cells generated in this structure were identified as neurons through their expression of TuJ1 (data not shown). Although at the level of the OT the ventral telencephalon had a large number of CB-ir cells (Fig. 7*O,P,Q*), none of the cells generated in the RMTW that followed either the ventral-medial or the dorsal-lateral routes expressed CB. However, the same proportion of migrating cells that used both routes (dorsal and ventral) weakly expressed Tbr1 (Fig. 7*I,Q*; 10.0%). Likewise, a similar yet higher percentage of cells in both populations express CR (Fig. 7*J–L,Q*; 46.3% the dorsal route and 50.6% the ventral route). However, the expression of Reln is different in these 2 populations as no more than 5.0% of the cells that course through the dorsal-lateral route express this protein, whereas 19.0% of the migrating cells in the ventral-medial route express Reln (Fig. 7*M,N,Q*).

Neuronal Migration of Double-Labeled Embryos: Final Topographical Setting in the OC

To identify the final location in the OC of the cell populations labeled after injection in the different telencephalic sites, several E11 mice were injected exo utero in 2 different telencephalic structures with different dyes (CFDA, SNARF-1) and cultured for 24 h in toto. Coronal sections throughout the rostrocaudal axis were studied to trace the final topography of the labeled cell populations in the OC that originated from the different telencephalic sources. The cell populations labeled in embryos injected in both the DT and SES areas (Fig. 8*A*) converged at the rostral (Fig. 8*B*) and medial (Fig. 8*C*) levels of the OC. Both cell populations occupied different OC areas and they overlapped at a small rostral region between the PC and OT (Fig. 8*D*). In fact, some labeled cells from the SES descended (as occurs in rostral and coronal sections) up to the septal area, whereas others ascended until they reached the border between the OT and PC. Caudally, labeled cells remained in the upper part of OT (Fig. 8*D,E*). Labeled cells from the RDT descended subpially up to the onset of the PC and rostrally, internally bordering this structure and separating the PC from the OT. At this point, there was some overlap between the cells coming from both sites, the SES and RDT. At caudal levels, the trajectory of the labeled cells from the MDT split at the dorsal limit of PC, and one branch migrated subpially, meanwhile the other one bordered the PC (Fig. 8*D,E*).

Embryos injected in the RMTW and SES were studied (Fig. 8*F*) to analyze the final rostral (Fig. 8*G*) and medial (Fig. 8*H*) distribution of the cells labeled from both the SES and the

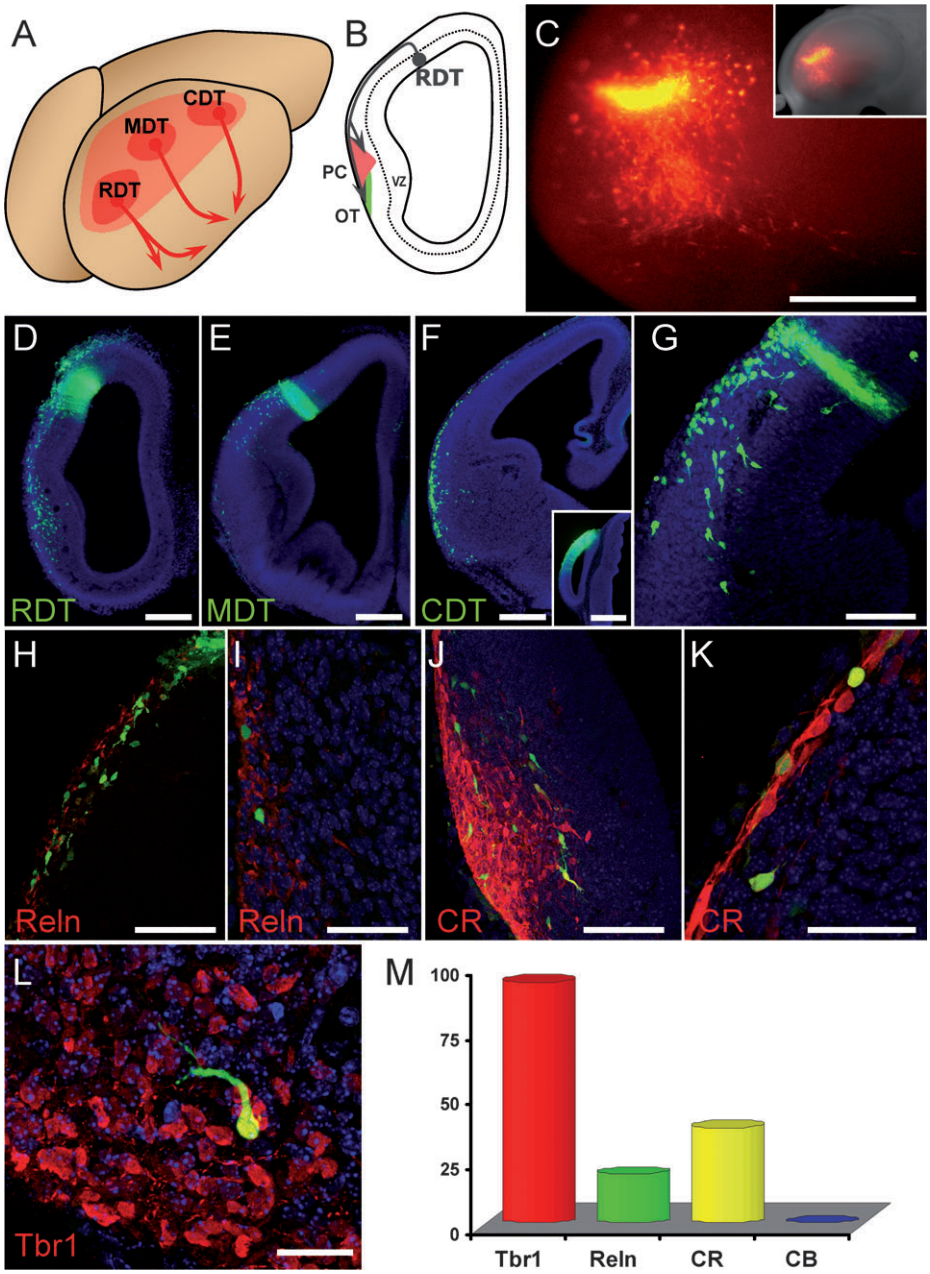

Figure 6. Neuronal migration from different areas of the DT. (*A*) Schematic drawing showing the extension of the DT (pale red) and the 3 different areas injected, rostral (RDT), medial (MDT), and caudal (CDT) part of this structure (red), with their migrating trajectories (red arrows). (*B*) Drawing of a coronal section at the rostral level showing the route followed by cells generated in the RDT that reach the PC and OT. vz, ventricular zone. (*C*) Photomicrography taken with a fluorescent dissecting microscope of a whole brain to show, from a lateral view, a DiI injection in RDT and the trajectory of the labeled cells. (*D*–*F*) Coronal sections showing injections of the green fluorescent compound CFDA in the rostral, medial, and caudal regions of this structure, respectively. (*G*) CFDA injection in MDT showing the bifurcation of the labeled stream of cells, at the level of the corticostriatal boundary. (*H*, *I*) Immunohistochemistry against Reelin (Reln, red) showing the immunoreactive subpial cells. The migrating DT cells are positioned in a deeper stratum of the PP (green). (*J*, *K*) Immunohistochemistry against calretinin (CR, red). These pictures show the external and internal distribution of DT-migrating cells (green) in the PC. Some of the green-labeled cells also express the CR-antibody (yellow). (*L*) Immunohistochemistry for Tbr1 (red) and double-labeled DT migrating neuron labeled with rhodamine (green). In order to maintain the same color in migrating cells all around the plate, we have changed the colors in this photo using Adobe Photoshop. (*M*) Bars diagram showing the percentage of cells expressing a given compound; Tbr1 (92.7%), Reln (18.8%), CR (36.7%), and CB (0.0%). Pictures (*D*–*G*) and (*I*–*L*) have been counterstained with bisbenzimide (blue). Scale bars: (*C*) and inset in (*F*), 500 μm; (*D*–*F*), 250 μm; (*G*, *H*, and *J*), 100 μm; (*I*, *K*), 50 μm; and (*L*), 25 μm.

ventromedial branch of the RMTW. Labeled cells from RMTW migrated over a subpial trajectory up to the most ventral part of the PC. Thus, this population passed through the area occupied by the SES-labeled cells and entered the PC area ventrally. In the overlapping areas, RMTW-labeled cells always run superficially to the SES-labeled cells, whereas there is also some overlap with RDT-labeled cells in the most ventral part of PC surface (Fig. 8*I*,*J*).

When embryos were injected in the DT (rostral or medial) (Fig. 8*K*) and the LGE (Fig. 8*L*), labeled cells from the main body of the LGE migrated radially to reach the upper layer of the PC. In their migratory route, these cells crossed the stream of the

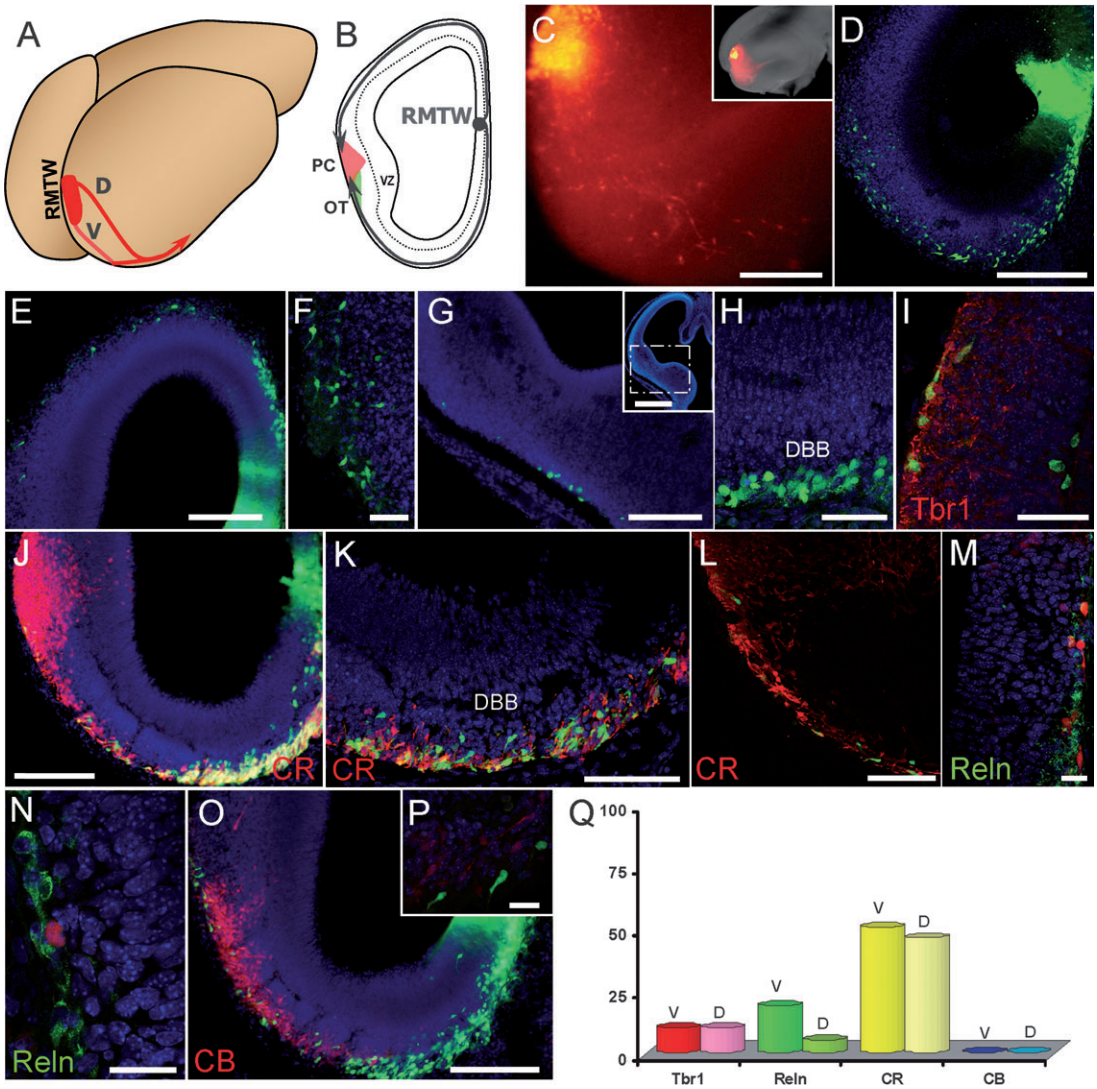

Figure 7. Neuronal migration from the RMTW. (*A*) Schematic drawing showing the injected region and the 2 divergent routes of migration found, dorsal (D) and ventral (V). Both routes converge rostrally in the OC where the cells migrate caudally (red arrow). (*B*) Drawing of a coronal and rostral section showing the injected area, the 2 divergent migratory routes (gray arrows) and the target region in the OC, the PC for the dorsal migration and the OT for the ventral migration. (*C*): Fluorescent photomicrograph of a DiI injection in RMTW in a whole brain, where the dorsal migratory route can be seen. (*D*) Coronal section displaying the CFDA-injection site (green) and the ventral migration that ends around the PC. (*E*) Coronal section showing part of the dorsal migration. (*F*) Enlargement of the OC area in a coronal section, adjacent to D, showing the morphology and orientation of labeled cells. (*G*) Caudal section (inset) displaying some CFDA-labeled cells in the caudal OC. (*H*) Labeled cells from the ventral migratory route, at the level of the DBB. (*I*) Coronal section immunostained for Tbr1 (red) showing single- and double-labeled cells coming from the ventral route. (*J–L*) Coronal sections immunostained for calretinin (CR, red) with CFDA-labeled cells from the ventral route, almost half of which are double labeled. (*M*, *N*) Coronal sections immunostained for Reelin (Reln, green) and Rho-labeled cells coming from the ventral (*M*) and dorsal (*N*) routes. (*O*, *P*) Coronal sections immunostained for calbindin (CB, red) and CFDA-labeled cells from the ventral route. (*Q*): Bar diagram showing the percentage of cells expressing a given compound: Tbr1 (V: 10.0%; D: 10.0%), Reln (V: 19.0%; D: 5.0%), CR (V: 50.6%; D: 46.3%), and CB (V and D: 0.0%). Pictures (*D–J* and *L–N*) have been counterstained with bisbenzimide (blue). Scale bars: (*C*) and inset in (*G*), 500 μm; (*D*), 250 μm; (*E*, *G*, *J*, and *O*), 200 μm; (*K*, *L*), 100 μm; (*F*, *H*, and *I*), 50 μm; and (*M*, *N*, and *P*), 25 μm.

internal branch of the DT-labeled cells, but they did not pass over the external branch of this population (Fig. 8*M–Q*).

Discussion

In this systematic study, we present evidence that at the earliest stages of mouse telencephalic development, different pallial germinative areas give rise to cell populations that express different markers and that migrate tangentially along stereotypic routes, topographically converging in the OC (Fig. 9). We also found 2 subpallial areas (the rLGE and the SES) that generate cells which migrate rostrally and incorporate into the pOB. Furthermore, it appears that the OC serves as a substrate for an important component of the tangential migratory stream in the rostrocaudal axis (Fig. 9*A*), in which distinct cell populations coexist and migrate simultaneously. Our observations are validated because the use of in toto embryo cultures allow us to trace the journey of the labeled cells from several injected regions, throughout different spatial telencephalic planes until they reach their target areas. As such, they are not subject to the limits or restraints on cellular movements that arise in slice cultures.

Cell Dynamics in the Early Telencephalon

There is much evidence that tangential migration is a generalized process in the earliest stages of telencephalic

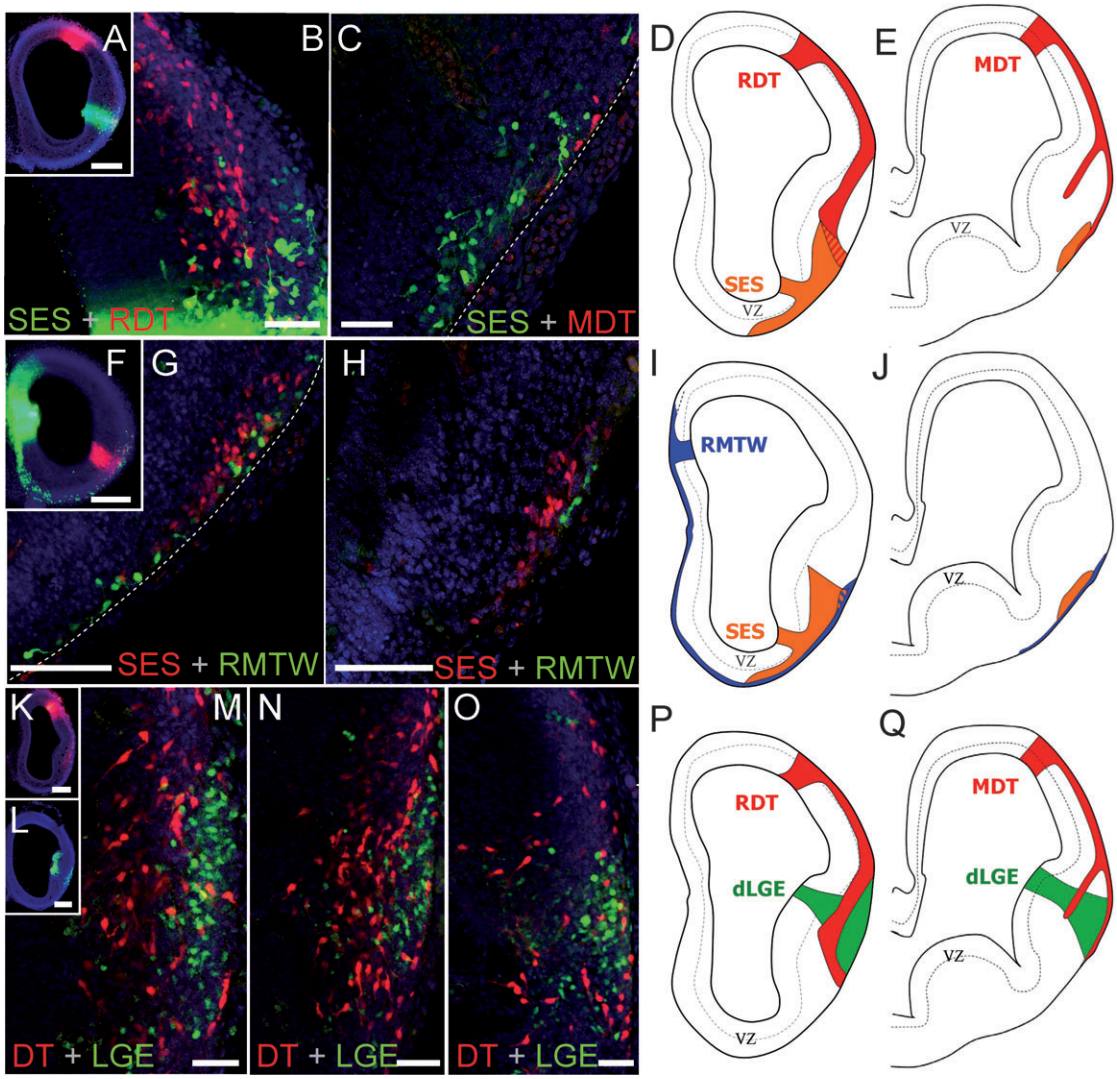

Figure 8. Topographical distribution of migrating cells in the OC. E11 embryos were double injected with both, CFDA (green) and SNARF-1 (red) in different parts of the telencephalon and cultured in toto for 24 h. Pictures in (*A–C*), (*F–H*), and (*K–O*) are coronal sections counterstained with bisbenzimide (blue) and showing diverse migrations according to the different injections sites. *D*, *E*, *I*, *J*, *P*, and *Q* are schematic drawings representing the topographical dispositions of each migratory cell population at the rostral and medial telencephalic levels. (*A*) SNARF-1 (red) injected in RDT and CFDA (green) injected in the SES. (*B*, *C*) show the disposition of labeled cells from both injection sites at rostral and medial levels, respectively. (*D*, *E*) summarize the complete trajectory of both labeled cell populations at the rostral (*D*) and medial (*E*) levels. (*F*) shows the injection sites in SES and in the RMTW; (*G*, *H*) show the final disposition at rostral and medial levels that have been summarized in the cartoons (*I* and *J*). Only the ventral migratory route from RMTW is represented. (*K*, *L*) show the injection sites in the RDT and in the dLGE. (*M–O*) show the final disposition, at different levels of the rostrocaudal axis, of the labeled cells. These dispositions are summarized in the cartoons (*P*, *Q*). In (*O*) and (*Q*), we can see the bifurcation of the RDT-labeled cells at medial levels. In the cartoons, vz is ventricular zone. Scale bars: (*A*, *F*, *K*, and *L*), 250 μm; (*G*, *H*), 100 μm; and (*B*, *C*, and *M–O*), 50 μm.

development. In fact, the cortical PP is now considered as an extraordinarily dynamic cellular layer that gives shelter to a series of migratory cell populations (Jiménez et al. 2002, Ang et al. 2003). One of these earliest populations are the Cajal-Retzius cells (Takiguchi-Hayashi et al. 2004; García-Moreno et al. 2007) that migrate tangentially through the upper part of neuroepithelium toward the lateroventral telencephalic region, following several precise migratory routes without surpassing the superior limit of the OC (Yoshida et al. 2006). However, there are other cell types that do not form part of the PP population but that rather use it as a migratory substrate, such as some GABAergic interneurons coming from the ganglionic eminences (Jiménez et al. 2002; Ang et al. 2003) and some cell populations related to the olfactory system (Tomioka et al. 2000; Nomura et al. 2006). In fact, primary olfactory cortical cells are among the first telencephalic neurons to differentiate as shown in tritiated thymidine (Hinds and Angevine 1965; Smart IHM and Smart M 1977; Bayer 1986; Valverde and Santacana 1994) and BrdU (De Carlos et al. 1996; Nomura et al. 2006) studies. However, in the present study, we demonstrate that these OC cells are generated in different parts of the developing telencephalon. Moreover, we investigate the possible role of the OC as an important early and crowded migratory highway (Fig. 9*A*), in accordance with previous studies describing the motility of embryonic OC cells (Hamasaki et al. 2001).

LGE-Derived Cells Colonize 3 Areas of the Olfactory System

A subpopulation of LGE-derived cells has been described that migrates to the OC (De Carlos et al. 1996; Wichterle et al. 2001;

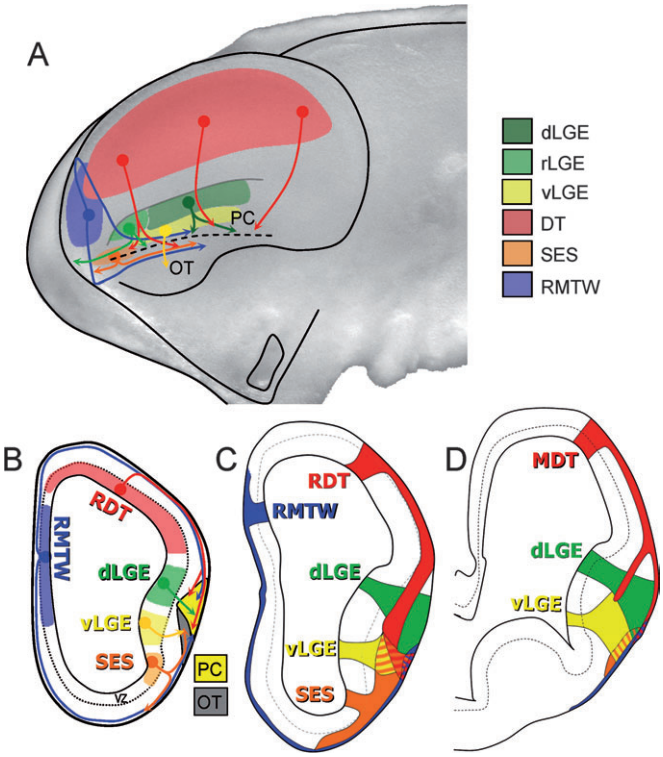

Figure 9. Cartoons representing the different areas of cell generation studied in the present work and the migratory routes identified in the complete brain (*A*) and in a coronal section (*B*). (*C*, *D*) represent the final topographical distribution of the different olfactory cell populations in the OC. The dorsal migration from the RMTW has not been represented, in order to avoid complicating the diagram, but this cell migration ended at the level of mid PC as did the RDT migration.

Legaz et al. 2005); however, the LGE has been subdivided into different domains based on genetic data (Puelles et al. 2000; Marín and Rubenstein 2002). Thus, although the dLGE domain is defined through the pattern of *Gsh2* expression (Corbin et al. 2000; Toresson and Campbell 2001), in the vLGE region both the *Gsh1* and *Gsh2* genes are expressed (Yun et al. 2003). Finally, we also considered the rLGE compartment because the *Er81* gene is expressed particularly in the rostrodorsal part of the LGE, where it colocalizes to a large extent with the subpallial *Dlx* genes (Yun et al. 2001; Stenman et al. 2003). Tracer injections into the rLGE at E11-labeled cells that migrate rostrally and tangentially to colonize the pOB (Fig. 9*A*). These cells appear to be related to those OB interneurons that express *Er81* (Stenman et al. 2003). We also show that cells generated in the dLGE migrate to exclusively occupy the PC, whereas the vLGE cells specifically colonize the OT (Fig. 9*B–D*). These data are in agreement with earlier results that correlated the development of the LGE with that of both the PC (De Carlos et al. 1996; Legaz et al. 2005) and the OT (Wichterle et al. 2001). However, our experimental approach does not allow to discriminate the migratory fate of 2 subpallial populations genetically different but that coexist in the corticostriatal border (CSB, Bielle et al. 2005; Carney et al. 2006). In this way, 3 different cell populations are generated in CSB at distinct temporal windows during embryogenesis (within a 2 day period), supplying cells to the PC and amygdala and to other basal telencephalic structures (Carney et al. 2006). Our data support the existence of 3 different areas in the same subpallial structure (LGE) that generate cells to populate diverse destinations in the olfactory system at the same embryonic age (E11). However, we cannot preclude the existence of others waves of cells generated at different embryonic ages, as described by Carney et al. (2006).

We describe 2 cell populations that migrate tangentially from the rLGE and SES toward the pOB at early stages, from E10 up to E12. The cells originating in the rLGE share features of OB interneurons (CR expression and subpalial origin) as well as features of projecting cells (Tbr1 expression and the lack of GAD-67 expression). In our experiments we have not differed between the ventral and dorsal portions of rLGE, and therefore, the high percentage of rLGE cells that expresses Tbr1 might suggest that the rostral migration arises only from the dorsal region of rLGE. Current evidence supports a model whereby OB-projection neurons require the activity of a specific set of transcription factors, including Tbr1 (Bulfone et al. 1998). Thus, given their expression of Tbr1, the time these cells arrive at the pOB and their initial horizontal disposition (Blanchart et al. 2006), it would appear that these cells are OB-projection cells, although their final fate remains to be confirmed. It has been proposed that OB-projecting cells (mitral cells) originate in the DT on the basis of Tbr1 expression as a pallial marker (Bulfone et al. 1998; Puelles et al. 2000). Alternatively, mitral cells have also been proposed to originate in the RDT (Nomura and Osumi 2004), a site compatible with our RMTW area. Thus, the migratory differences described above generate some uncertainty about the actual origin of mitral cells, and additional studies will be needed to better understand this issue. On other hand, based on the expression of CB and the lack of both Reln and Tbr1, cells originating in the SES could produce the first interneuron cell population that tangentially reaches the pOB.

The Dorsal and Medial Telencephalon Contributes to the Formation of the OC

Cells generated in different areas of the DT migrate through the lower part of the PP, avoiding the upper part occupied by horizontal Reln-positive cells (Hevner et al. 2003). These DT cells reach the OC where they settle at the border of the PC, whereas the lot becomes encircled by the so-called lot cells that migrate ventrally from the dorsal telencephalic vesicle (Sato et al. 1998; Tomioka et al. 2000; Kawasaki et al. 2006). Thus, based on their different morphologies, location, and immunohistochemical properties, we rule out the possibility that DT-generated cells are lot cells. In contrast, a cell population other than lot cells descends from the DT to halt their migration, through Eph A5–Pax6 signaling, in the deepest areas of the OC (Nomura et al. 2006). This population is similar to that described in the current work, although there are differences such as the lack of CB expression in the pallium at early developmental stages. In fact, the expression of this protein begins after the arrival of GABAergic cells from the basal telencephalon (Anderson et al. 1997; Jiménez et al. 2002). However, the cells described by Nomura et al. (2006) strongly express CB and Reln, whereas the dorsally generated cells that migrate by the PP and express Reln are Cajal-Retzius cells and they do not express CB (Ogawa et al. 1995; Schiffmann et al. 1997; Meyer and Goffinet 1998; García-Moreno et al. 2007). Our experiments show that the cells generated in the RMTW reach the OC by different migratory routes (Fig. 9*A*). This is a region equivalent to that described by Nomura and Osumi (2004) where they located a potential site of mitral cell origin.

Using similar experimental procedures to ours, Nomura and Osumi failed to observe a tangential component of the cells generated in that region, except in the sey mutants. However, after performing injections in wild-type embryos, we found dorsal tangential migration similar to that described in the Pax6 mutant, together with a large cell population that migrate along the subpalial region and settle in the OT. Interestingly, the cells that follow the ventral route seem to populate the DBB, which extends the number of telencephalic structures that receive cells by tangential migration.

As a general rule, the data presented indicate that cells generated in the pallium migrate tangentially along both the dorsoventral and caudorostral axis. In contrast, those generated in the subpallium migrate, mainly along the rostrocaudal axis, using the OC as substratum. As an exception, most cells generated in rLGE and SES migrates rostrally through the subpallium to reach pOB. Finally, pallial-generated cells migrate caudally just when they cross the CSB.

Our results also provide additional evidences that neuronal diversity and regionalization are established already prior to the migration of newborn neurons, as suggested by classical protomap hypothesis (Rakic 1988; López-Mascaraque and de Castro 2002; Mallamaci and Stoykova 2006; Cholfin and Rubenstein 2007). This is also consistent with a recent study (Merkle et al. 2007), which show that different regions of the subventricular zone give rise to different types of olfactory neurons, suggesting the possibility that the activity of neural stem cells is regionally modulated in order to regulate the production of different types of neurons.

In summary, our study highlights the importance of the neuronal tangential migration as a widespread process at the earliest stages of telencephalic development. We show that olfactory-related neurons that converge in the OC are generated at multiple sites across the entire telencephalon (Fig. 9*B–D*). This strategy might contribute to the diversity of the OC neurons. Interestingly, a subpopulation of LGE and SES cells also migrate tangentially toward the pOB, and cells from the medial pallium colonize the DBB and reach the OC following opposite routes. In conclusion, pallial migration occurs in a rostral direction, whereas subpallial does in caudal direction (Fig. 9*A*), with the exception of some structures such as the rLGE and SES, whose cells migrate rostrally. It will now be of interest to determine the factors that are involved in orchestrating these migratory pathways, both those at their origin and in their target areas.

Supplementary Material

Supplementary figure S1 can be found at: http://www.cercor.oxfordjournals.org/.

Funding

Spanish Ministerio de Educación y Ciencia (BFU2006–01898); the OLFACTOSENSE Consortium, Comunidad Autónoma de Madrid (P-SEM-0255-2006).

Notes

We thank M[a] Laura Ceci, Albert Blanchart, and Jorge García-Marqués for helpful comments on the manuscript, Mark Sefton for editorial assistance and Nieves Salvador for technical support. *Conflict of Interest:* None declared.

Address correspondence to email: decarlos@cajal.csic.es.

References

Anderson SA, Eisenstat DD, Shi L, Rubenstein JLR. 1997. Interneuron migration from basal forebrain to neocortex: dependence on Dlx genes. Science. 278:474–476.

Ang ESB, Tarik FH, Gluncic V, Rakic P. 2003. Four-dimensional migratory coordinates of GABAergic interneurons in the developing mouse cortex. J Neurosci. 23:5805–5815.

Bayer SA. 1986. Neurogenesis in the rat primary olfactory cortex. Int J Neurosci. 4:251–271.

Bielle F, Griveau A, Narboux-Neme N, Vigneau S, Sigrist M, Arber S, Wassef M, Pierani A. 2005. Multiple origins of Cajal-Retzius cells at the borders of the developing pallium. Nat Neurosci. 8:1002–1012.

Blanchart A, De Carlos JA, López-Mascaraque L. 2006. Time frame of mitral cell development in the mice olfactory bulb. J Comp Neurol. 496:529–543.

Brunjes PC, Illing KR, Meyer EA. 2005. A field guide to the anterior olfactory nucleus (cortex). Brain Res Rev. 50:305–335.

Bulfone A, Wang F, Hevner R, Anderson S, Cutforth T, Chen S, Meneses J, Pedersen R, Axel R, Rubenstein JL. 1998. An olfactory sensory map develops in the absence of normal projection neurons or GABAergic interneurons. Neuron. 21:1273–1282.

Carney RS, Alfonso TB, Cohen D, Dai H, Nery S, Stoica B, Slotkin J, Bregman BS, Fishell G, Corbin JG. 2006. Cell migration along the lateral cortical stream to the developing basal telencephalic limbic system. J Neurosci. 26:11562–11574.

Cholfin JA, Rubenstein JL. 2007. Patterning of frontal cortex subdivisions by Fgf17. Proc Natl Acad Sci USA. 104:7652–7657.

Corbin JG, Gaiano N, Machold RP, Langston A, Fishell G. 2000. The Gsh2 homeodomain gene controls multiple aspects of telencephalic development. Development. 127:5007–5020.

De Carlos JA, López-Mascaraque L, Valverde F. 1996. Dynamics of cell migration from the lateral ganglionic eminence in the rat. J Neurosci. 16:6146–6156.

De Carlos JA, O'Leary DDM. 1992. Growth and targeting of subplate axons and establishment of major cortical pathways. J Neurosci. 12:1194–1211.

Francis F, Koulakoff A, Boucher D, Chafey P, Schaar B, Vinet MC, Friocourt G, McDonnell N, Reiner O, Kahn A, *et al.* 1999. Doublecortin is a developmentally regulated, microtubule-associated protein expressed in migrating and differentiating neurons. Neuron. 23:247–256.

García-Moreno F, López-Mascaraque L, De Carlos JA. 2007. Origins and migratory routes of murine Cajal-Retzius cells. J Comp Neurol. 500:419–432.

Gleeson JG, Lin PT, Flanagan LA, Walsh CA. 1999. Doublecortin is a microtubule-associated protein and is expressed widely by migrating neurons. Neuron. 23:257–271.

Haberly LB. 2001. Parallel-distributed processing in olfactory cortex: new insights from morphological and physiological analysis of neuronal circuitry. Chem Senses. 26:551–576.

Hamasaki T, Goto S, Nishikawa S, Ushio Y. 2001. Early-generated preplate neurons in the developing telencephalon: inward migration into the developing striatum. Cereb Cortex. 11:474–484.

Hevner RF, Neogi T, Englund C, Daza RAM, Fink A. 2003. Cajal–Retzius cells in the mouse: transcription factors, neurotransmitters, and birthdays suggest a pallial origin. Dev Brain Res. 141:39–53.

Hinds JW, Angevine JB. 1965. Autoradiographic study of the histogenesis in area pyriformis and claustrum in mouse. Anat Rec. 151:456.

Hof PR, Glezer II, Condé F, Flagg RA, Rubin MB, Nischinsky EA, Vogt Weisenhorn DM. 1999. Cellular distribution of the calcium-binding proteins parvalbumin, calbindin, and calretinin in the neocortex of mammals: phylogenetic and developmental patterns. J Chem Neuroanat. 16:77–116.

Jiménez D, López-Mascaraque LM, Valverde F, De Carlos JA. 2002. Tangential migration in neocortical development. Dev Biol. 244:155–169.

Jiménez D, Rivera R, López-Mascaraque L, De Carlos JA. 2003. Origin of the cortical layer I in rodents. Dev Neurosci. 25:105–115.

Kawasaki T, Ito K, Hirata T. 2006. Netrin 1 regulates ventral tangential migration of guidepost neurons in the lateral olfactory tract. Development. 133:845–853.

Lavdas AA, Grigoriou M, Pachnis V, Parnavelas JG. 1999. The medial ganglionic eminence gives rise to a population of early neurons in the developing cerebral cortex. J Neurosci. 15:7881–7888.
Lee MK, Tuttle JB, Rebhun LI, Cleveland DW, Frankfurter A. 1990. The expression and posttranslational modification of a neuron-specific β-tubulin isotype during chick embryogenesis. Cell Motil Cytoskeleton. 17:118–132.
Legaz I, García-Lopez M, Medina L. 2005. Subpallial origin of part of the calbindin-positive neurons of the claustral complex and piriform cortex. Brain Res Bull. 66:470–474.
Lois C, Alvarez-Buylla A. 1994. Long distance neuronal migration in the adult mammalian brain. Science. 264:1145–1148.
López-Bendito G, Sturgess K, Erdelyi F, Szabo G, Molnar Z, Paulsen O. 2004. Preferential origin and layer destination of GAD65-GFP cortical interneurons. Cereb Cortex. 14:1122–1133.
López-Mascaraque L, De Carlos JA, Valverde F. 1996. Early onset of the rat olfactory bulb projections. Neuroscience. 70:255–266.
López-Mascaraque L, de Castro F. 2002. The olfactory bulb as an independent developmental domain. Cell Death Differ. 9: 1279–1286.
Mallamaci A, Stoykova A. 2006. Gene networks controlling early cerebral cortex arealization. Eur J Neurosci. 23:847–856.
Marín O, Rubenstein JLR. 2002. Patterning, regionalization and cell differentiation in the forebrain. In: Rossant J, Tam P, editors. Mouse development. San Diego (CA): Academic Press. p. 75–106.
Marín-Padilla M. 1971. Early prenatal ontogenesis of the cerebral cortex (neocortex) of the cat (Felis domestica). A golgy study. I. The primordial neocortical organization. Z Anat Entwicklungsgesh. 134:117–145.
Marín-Padilla M. 1978. Dual origin of the mammalian neocortex and evolution of the cortical plate. Anat Embryol. 153:109–126.
Merkle FT, Mirzadeh Z, Alvarez-Buylla A. 2007. Mosaic organization of neural stem cells in the adult brain. Science. 317:381–384.
Meyer G, Goffinet AM. 1998. Prenatal development of reelin-immunoreactive neurons in the human neocortex. J Comp Neurol. 397:29–40.
Nomura T, Holmberg J, Frisen J, Osumi N. 2006. Pax6-dependent boundary defines alignment of migrating olfactory cortex neurons via the repulsive activity of ephrin A5. Development. 133: 1335–1345.
Nomura T, Osumi N. 2004. Misrouting of mitral cell progenitors in the Pax6/small eye rat telencephalon. Development. 131:787–796.
Ogawa M, Miyata T, Nakajima K, Yagyu K, Seine M, Ikenaka K, Yamamoto H, Mikoshiba K. 1995. The reeler gene-associated antigen on Cajal-Retzius neurons is a crucial molecule for laminar organization of cortical neurons. Neuron. 14:899–912.
Puelles L, Kuwana E, Puelles E, Bulfone A, Shimamura K, Keleher J, Smiga S, Rubenstein JL. 2000. Pallial and subpallial derivatives in the embryonic chick and mouse telencephalon, traced by the expression of the genes Dlx-2, Emx-1, Nkx-2.1, Pax-6, and Tbr-1. J Comp Neurol. 424:409–438.
Rakic P. 1972. Mode of cell migration to the superficial layers of the fetal monkey neocortex. J Comp Neurol. 145:61–84.
Rakic P. 1988. Specification of cerebral cortical areas. Science. 241:170–176.
Sato Y, Hirata T, Ogawa M, Fujisawa H. 1998. Requirement for early-generated neurons recognized by monoclonal antibody lot1 in the formation of lateral olfactory tract. J Neurosci. 18:7800–7810.
Schiffmann SN, Bernier B, Goffinet AM. 1997. Reelin mRNA expression during mouse brain development. Eur J Neurosci. 9:1055–1071.
Smart IHM, Smart M. 1977. The location of nuclei of different labeling intensities in autoradiographs of the anterior forebrain of postnatal mice injected with ^{3}H-tymidine on the eleventh and twelfth days post-conception. J Anat. 123:515–525.
Stenman J, Toresson H, Campbell K. 2003. Identification of two distinct progenitor populations in the lateral ganglionic eminence: implications for striatal and olfactory bulb neurogenesis. J Neurosci. 23: 167–174.
Stewart GR, Pearlman AL. 1987. Fibronectin-like immunoreactivity in the developing cerebral cortex. J Neurosci. 7:3325–3333.
Takiguchi-Hayashi K, Sekiguchi M, Ashigaki S, Takamatsu M, Hasegawa H, Suzuki-Migishima R, Yokoyama M, Nakanishi S, Tanabe Y. 2004. Generation of reelin-positive marginal zone cells from the caudomedial wall of telencephalic vesicles. J Neurosci. 24:2286–2295.
Tamamaki N, Fujimori E, Takauji R. 1997. Origin and route of tangentially migrating neurons in the developing neocortical intermediate zone. J Neurosci. 17:8313–8323.
Tomioka N, Osumi N, Sato Y, Inoue T, Nakamura S, Fujisawa H, Hirata T. 2000. Neocortical origin and tangential migration of guidepost neurons in the lateral olfactory tract. J Neurosci. 20:5802–5812.
Toresson H, Campbell K. 2001. A role for Gsh1 in the developing striatum and olfactory bulb of Gsh2 mutant mice. Development. 128:4769–4780.
Valverde F. 1965. Studies on the piriform lobe. Cambridge (MA): Harvard University Press.
Valverde F, Santacana M. 1994. Development and early postnatal maturation of the primary olfactory cortex. Brain Res Dev Brain Res. 80:96–114.
Wichterle H, Turnbull DH, Nery S, Fishell G, Alvarez-Buylla A. 2001. In utero fate mapping reveals distinct migratory pathways and fates of neurons born in the mammalian basal forebrain. Development. 128: 3759–3771.
Yoshida M, Assimacopoulos S, Jones KR, Grove EA. 2006. Massive loss of Cajal-Retzius cells does not disrupt neocortical layer order. Development. 133:537–545.
Yun K, Garel S, Fischman S, Rubenstein JL. 2003. Patterning of the lateral ganglionic eminence by the Gsh1 and Gsh2 homeobox genes regulates striatal and olfactory bulb histogenesis and the growth of axons through the basal ganglia. J Comp Neurol. 461:151–165.
Yun K, Potter S, Rubenstein JL. 2001. Gsh2 and Pax6 play complementary roles in dorsoventral patterning of the mammalian telencephalon. Development. 128:193–205.